JOURNAL OF THE KOREAN ASTRONOMICAL SOCIETY
37: 185 ~ 191, 2004

CHARACTERISTICS AND PERFORMANCE OF A FAST CCD CAMERA: DALSTA IM30P

YOUNG-MIN SEO, KI-WOONG PARK, AND JONGCHUL CHAE
Astronomy Program, School of Earth and Environmental Sciences, Seoul 151-742, Korea
(Received December 1, 2004; Accepted December 24, 2004)

ABSTRACT

We have been developing a solar observing system based on a fast CCD camera 1M30P made by the DALSA company. Here we examine and present the characteristics and performance of the camera. For this we have analyzed a number of images of a flat wall illuminated by a constant light source. As a result we found that in the default operating mode 1) the mean bias level is 49 ADU/pix, 2) the mean dark current is about 8 ADU/s/pix, 3) the readout noise is 1.3 ADU, and 4) the gain is about 42 electrons/ADU. The CCD detector is found to have a linearity with a deviation smaller than 6 %, and a uniform sensitivity better than 1%. These parameters will be used as basic inputs in the analysis of data to be taken by the camera.

Key words : astronomical instrumentation: CCD camera - solar observation

I. INTRODUCTION

Solar observations are distinguished from nighttime observations in that the time of light exposure is very short, typically sub-seconds. An obvious reason coming from an observational point of view is that the Sun is close and bright enough, that is, it has enough number of photons. Another observational reason is relevant to the astronomical seeing. Daytime observations are easily subject to the seeing since the heating by the solar radiation drives atmospheric turbulence. A way of minimizing the degradation effect by the seeing is to take a very short exposure and capture almost still images of moving features. The short exposure is preferred from a scientific point of view, too. There are many solar features of scientific interests changing rapidly with time, like flares. Their time scale ranges from a few minutes down to a few miliseconds. High cadence observations with short exposures is crucial for the study of this kind of features (e.g., Wang et al. 2000; Hanaoka et al. 2004).

We have been developing a solar observing system based on a fast CCD camera which is characterized by short exposures and fast data transfer. The purpose of the present paper is to examine its characteristics and performance that may be much different from the traditional astronomical CCD camera used in nighttime observations. We specifically intend to determine the bias, dark current, gain, readout noise, linearity and so on, which will serve as basic inputs for the future observational studies.

II. OBSERVING SYSTEM

The observing system consists of a CCD camera, a frame grabber, and a control computer equipped with Microsoft Visual C++. The camera used in our system is a DALSTAR 1M 30P camera (Figure 1) manufactured by DALSA Corporation, USA. It is a 12-bit, frame transfer 1024×1024 CCD camera with a frame rate of 30 fps. The physical size of each CCD pixel is 12μm x 12μm and the detector has an area of 12.3mm x 12.3mm. The quantum efficiency is about 20 % at the Hα wavelength.

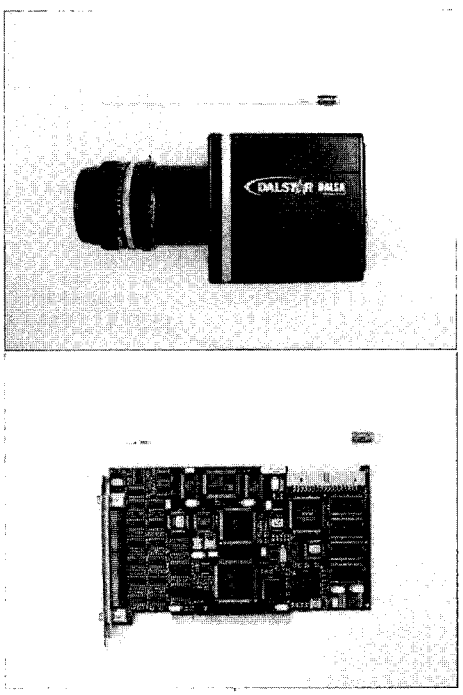

Fig. 1.— 1M30P CCD camera and NI PCI-1422 frame grabber (courtesy of Hyung-Min Park).

We have developed a software written in Microsoft

Corresponding Author: J. Chae

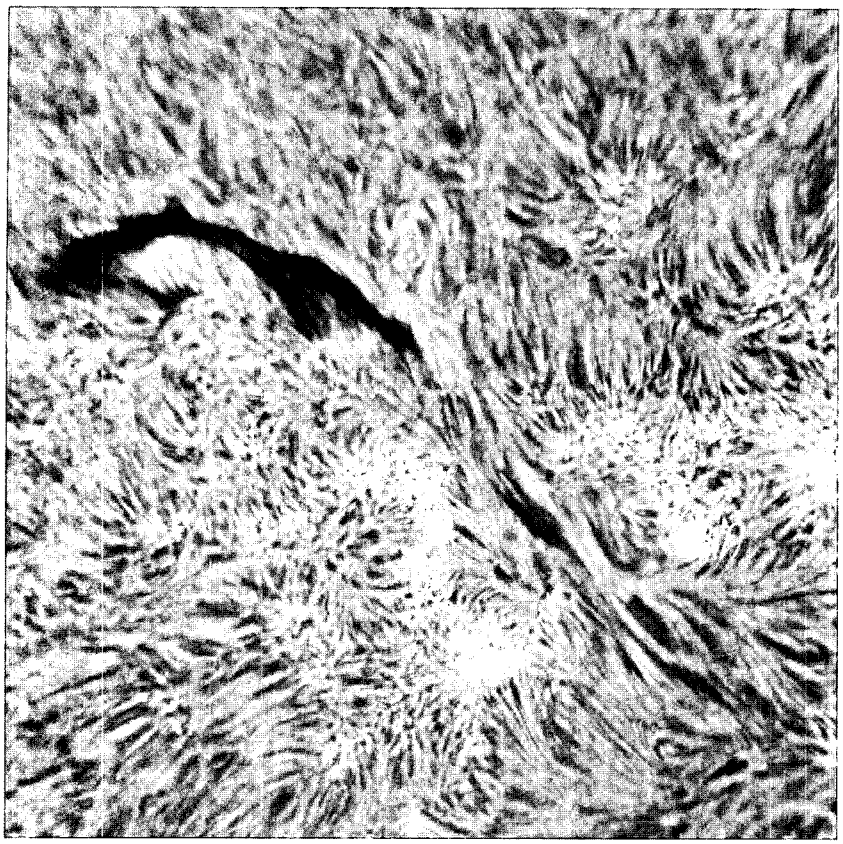

Fig. 2.— An Hα image of a region on the solar surface taken with the 1M30P camera.

Visual C++ to control the camera and acquire data. The software communicates with the camera via a serial port and controls the parameters of the camera such as exposure time, gain, frame per second, and binning. The data acquisition is done with the aid of a frame grabber. We use the PCI-1422 frame grabber made by the National Instruments Corporation (see Figure 1). This has a 40 MHz clock speed, and digitizes the data in 16 bit. It comes with the IMAQ driver, a set of basic C functions. These functions can be used to control buffer management, signal I/O, and data acquisition.

Figure 2 shows one of the solar images taken with the camera. The observation was performed on 2004 August 3 using the 10 inch refractor and the Zeiss Hα filter of the Big Bear Solar Observatory. The wavelength of the filter was set to the center of the Hα line. The image shows a filament and its associated filament channel.

III. PRINCIPLE OF DATA ANALYSIS

(a) Principle

The strength of the light signal measured at each CCD pixel is commonly expressed in analog-to-digital unit (ADU). Let denote o_i as the signal (in unit of ADU/s) to be recorded at the i-the pixel of an ideal detector with zero bias and zero dark current. Then the signal $p_{i,t}$ (in unit of ADU) recorded at the same pixel of a real detector for t seconds can be expressed as

$$p_{i,t} = o_i f_i t + d_i t + b_i + n_i \quad (1)$$

where b_i is the bias (in unit of ADU), d_i, dark current (in unit of ADU/s), and f_i, the flat pattern which represents the relative response of each pixel to a uniform illumination. Note that Equation 1 basically assumes the linearity of the detector to the integrated signal. We will later examine this linearity. The added term n_i represents the noise in the measurement.

Different sources may contribute to the noise $\sigma(n_i)$, which include the read-out noise $\sigma_{R,i}$, photon noise $\sigma_{P,i}$ and other unknown noise $\sigma_{U,i}$, so we can write down

$$\sigma^2(n_i) = \sigma^2_{R,i} + \sigma^2_{P,i} + \sigma^2_{U,i}\,. \quad (2)$$

(b) Data Analysis

To handle with the noise in the measurement, we take a set of images with the same condition imposed, to form an ensemble. We denote an ensemble average by $\langle\ \rangle$, and it is natural to assume

$$\langle n_i \rangle = 0. \quad (3)$$

Then we find from Equation 1

$$\langle p_{i,t} \rangle = o_i f_i t + d_i t + b_i \tag{4}$$

and

$$\sigma^2(n_i) = \langle (p_{i,t} - \langle p_{i,t} \rangle)^2 \rangle \tag{5}$$

Note in the right-hand side of Equation 4 the notation $\langle\ \rangle$ has been omitted since the ensemble averages of noise-free terms are equal to themselves by definition, that is, $\langle o_i f_i t \rangle = o_i f_i t$, $\langle d_i t \rangle = d_i t$ and so on.

(c) Determination of Bias, Dark Current, and Readout noise

If we choose $t = 0$, then we can determine the bias

$$b_i = \langle p_{i,0} \rangle \tag{6}$$

and the square sum of the readout noise and the unknown noise

$$\sigma^2_{R,i} + \sigma^2_{U,i} = \langle (p_{i,0} - \langle p_{i,0} \rangle)^2 \tag{7}$$

from the ensemble of p_i. But it is technically not allowed to set t exactly to zero. Alternatively we take several sets of ensembles with different exposures with the incoming light blocked. Then we obtain the relation to be used to derive d_i and b_i from the data

$$d_i t + b_i = \langle p_{i,t} \rangle \tag{8}$$

and the expression for the readout noise

$$\sigma^2_{R,i} \leq \langle (p_{i,t} - \langle p_{i,t.} \rangle)^2 \rangle \tag{9}$$

Note that the readout noise is expected to be independent of t, and is not greater than the measured noise.

We made use of Equation 8 to determine d_i and b_i separately. The required data are a set of $\langle p_{i,t} \rangle$ with different exposure time t. The first order polynomial fit yields bias b_i and dark current d_i at every pixel.

(d) Determination of Gain

It is well known that the photon noise expressed in electrons is given by the square root of the signal expressed in electrons. The conversion from electrons to ADU or vice versa can be done with the help of gain g which is normally expressed in unit of electrons/ADU. We require that the gain should not depend on the pixel. Then the photon noise expressed in ADU is given by

$$\sigma^2_{P,i} = o_i f_i t / g. \tag{10}$$

This expression may be written in the form

$$o_i f_i t = g \sigma^2_{P,i}. \tag{11}$$

Once we determine d_i, b_i, it is possible to determine $o_i f_i t$ for each t from Equation 4. The corresponding noise $\sigma_{P,i}$ for each t can be determined from Equations 2 and 5 if $\sigma_{R,i}$ is already known and $\sigma_{U,i}$ is assumed to be zero. The slope of the plot of $o_i f_i t$ over $\sigma^2_{P,i}$ will yield the gain g. The gain, by our definition, should not depend on the pixel, but it may, because of the uncertainty in measurements. So we determine the gain at every pixel, but take only its average as the final value. The detailed knowledge on the calculation of readout noise and gain can be found in the CCD text books like Howell (2000).

IV. RESULTS

(a) Experiments

The experiments were performed in a laboratory. We have recorded a number of images of a flat wall illuminated by a commercial light bulb. Since the voltage is modulated alternately at a frequency of 60 Hz, the light level may change at a short time scale. Hence a set of images taken with random grabbing show significant fluctuation in light level, not being suited for an ensemble. We solved this problem by taking a sequence of images at the cadence of 1/30 second, which is exactly twice the modulation period of the voltage. As a result we found no noticeable difference in light level among the images. Thus this set of images are suited for an ensemble.

(b) Effective Integration Time Range

According to the camera manual provided by the DALSA Corporation, it is possible in principle to set the exposure time in 18 bit integers of microseconds, that is, from 0 to 262143 microseconds. But we found that the practically effective range of the integration time is from 5 to 210 miliseconds. The lower bound suggested by the camera manual is 2.16 miliseconds which is to minimize the effect of finite readout time. We have found the upper bound experimentally. When longer exposures are taken, images become too smeared in one direction to be used. The images look like those taken with exposures shorter than 5 miliseconds, so we suspect that there is a camera operation error we do not understand.

(c) Bias, Dark Current, Readout Noise

Based on Equation 8, we have determined bias and dark current at every pixel. We used 42 steps of integration time from 5 miliseconds to 210 miliseconds. A set of 50 images were taken at each integration time to form an ensemble.

Figure 3 shows the bias image. It is seen from the figure that about 30 columns near the left edge have either abnormally big values up to 665 ADU, or abnormally small values down to 0 ADU. With these abnormal columns excluded, the mean value of bias is found to be 48.5 ADU, and the pixel-to-pixel standard variation is 0.3 ADU. This standard value seems to mostly reflect the pattern of column-to-column variation.

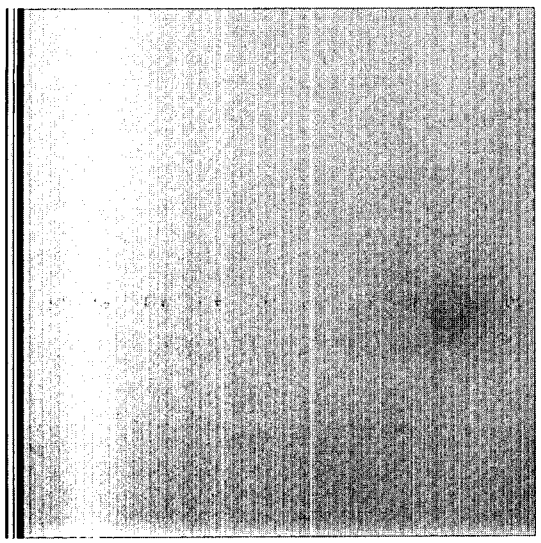

Fig. 3.— The bias image.

We have found that determining the dark current at every pixel is hampered by the too short range of integration time as can be seen from Equation 8. The only meaningful value we can provide should be a representative of the dark current for all the pixels, namely its spatial average value. The value is 8 ADU/s.

We have estimated the readout noise using Equation 9. As a matter fact, the right hand side of Equation 9 is not only contributed by the readout noise, but also by the noise associated with the fluctuation of dark current, which is a kind of Poisson noise. The former is independent of integration time, but the latter is not. The dark current-associated noise is expected to increase with integration time. We have tested how significant this noise is by varying the integration time. With the short integration of 5 miliseconds, the standard noise is found to be 1.32 ADU, and its spatial fluctuation, 0.15 ADU excluding the abnormal columns. With the longer integration of 210 miliseconds, the standard noise is found to be 1.38 ± 0.30 ADU. The difference in the measured noise between the two integration is very small. Therefore we conclude that the contribution of dark current to the noise is not significant and the readout noise is about 1.3 ADU. This value is not much different from the system noise of 1.5 ADU specified in the camera manual.

(d) Linearity

In principle the linearity of the detector should be tested by varying the intensity of the light incident on the detector. But this is practically impossible for us to do because we have no light source of which intensity we can control with a good accuracy. Alternatively, we use a constant light source and change the exposure time, and examine how the output signal depends on the exposure time. If the detector is linear, the measured signal with the bias subtracted should be proportional to the exposure time.

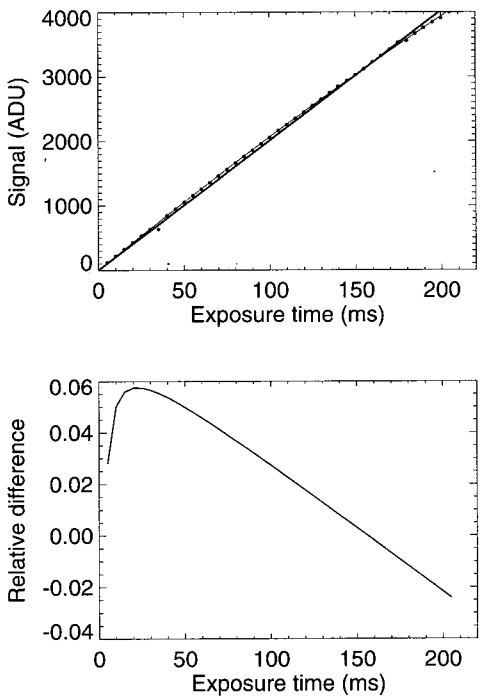

Fig. 4.— The upper panel: The signal of a constant light source recorded by a pixel as a function of time (symbols). The standard deviation error in the signal is smaller than the size of the symbols. The thick solid line is the linear fit to the data, and the the thin curve is a non-linear (2nd order polynomial) fit. The lower panel: The relative difference defined by the difference between the non-linear fit and the linear fit divided by the linear fit.

Figure 4 illustrates the result of our test obtained at an arbitrarily chosen pixel. The exposure time-signal curve has a small dip near an exposure of 35 ms. This dip appeared in some experiments, but not in other experiments. So far we have no definite clue to understanding the character of this dip. To examine the possible non-linearity of the pixel while minimizing the effect of the noise, we have applied a non-linear (2nd order polynomial) fit to the data, and compared with the linear fit. The relative difference between the two fits provides us with a measure of deviation from linearity. From the figure we find that the pixel is linear better than an accuracy of 6%. We have examined the linearity in other pixels, and obtained similar results.

(e) Gain

We have determined the gain (electrons/ADU) using two different sets of data. One set was obtained without binning, the other with 1×2 binning. The upper panel of Figure 5 is an example of gain determination at a pixel using the data without binning. The gain at this

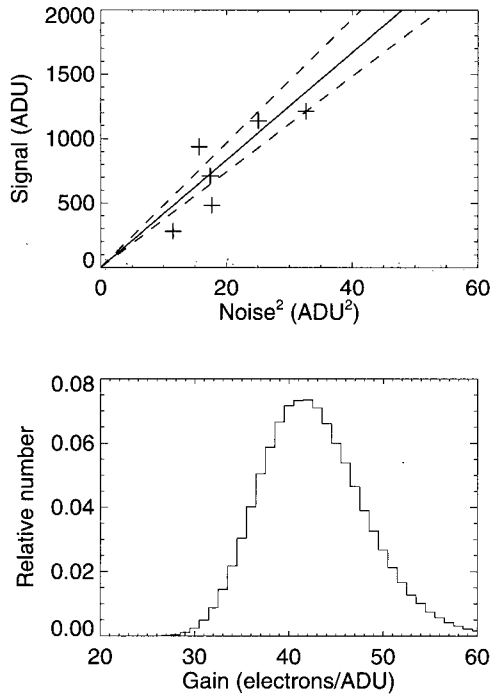

Fig. 5.— Upper panel: an example of a linear fit to the noise square-signal relation at a pixel. The solid line is the best fit, of which slope is found to be the gain. Lower panel: the number distribution of gain. The mean value is 42.7 electrons/ADU and the standard deviation is 5.6 electrons/ADU. The slopes of the two dashed lines in the upper panel are (42.7 ± 5.6) electrons/ADU, respectively.

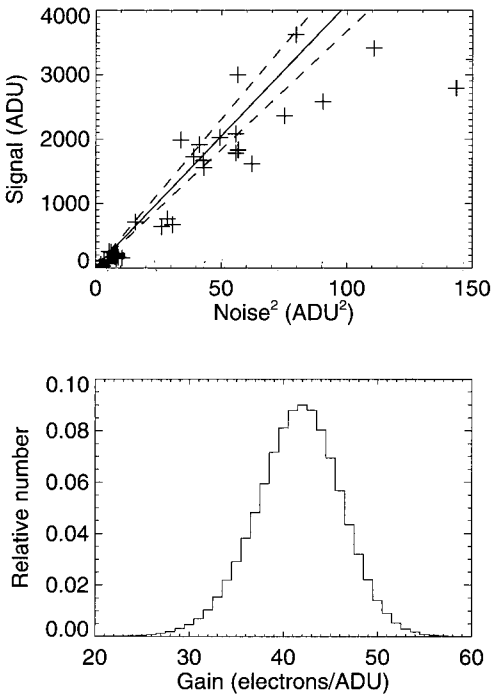

Fig. 6.— The same as Fig. 5, but using data with 1 × 2 binning. The mean value is 41.5 electrons/ADU and the standard deviation is 4.7 electrons/ADU. The slopes of the two dashed lines in the upper panel are (41.5 ± 4.7) electrons/ADU, respectively.

pixel is measured to be 41.7 electrons/ADU. We have examined the gain at every pixel of the detector. The low panel shows the number distribution of the gain. Its mean value is 42.7 electrons/ADU and its standard deviation is 5.6 electorns/ADU. The two dashed lines with the slopes (42.7 ± 5.6) electrons/ADU are consistent with the data at the pixel within the measurement error. Thus it is likely that the variation of the gain represents the errors in the measurement rather than the true pixel-to-pixel variation.

Figure 6 shows a similar result obtained using the binned data set. Applying binning turns out effective in increasing the signal level. But we find that the binned data may have additional unknown noise. For example, at this pixel, different measurements of the signal with about the same level of 2800 ADU accompany noises of different magnitudes ranging from $60^{1/2}$ to $140^{1/2}$ ADU. We think the the bigger ones contain unknown noise in addition to the photon noise. At present we do not understand the physical origin of this unknown noise, but we imagine the binning process might be introducing some electronic noise. To minimize the effect of this additional noise, we used only the measurements with noise less than a critical value. We found that choosing $60^{1/2}$ ADU resulted in the gain distribution that is similar to the one we obtained from the data without binning (see the figiure).

(f) Adjusting Gain

The camera allows users to adjust the gain. The gain is adjustable from 1 to 10 by writing a 16 bit integer via RS-232 serial interface, so that the number of allowed gain steps is 32768. The data number expressed in ADU with a choice of, for example, 5x gain is expected to be five times that of the 1x gain case. Therefore, the output gain defined in unit of electrons/ADU should be inversely proportional to the input gain step (in this case 5). We have checked this prediction by determining the gains for different gain steps.

Figure 7 presents our result. Ideally the output gain should be inversely proportional to the input gain step as illustrated by the straight line. The figure shows the output gain is roughly inversely proportional to the input gain step when the gain step is not bigger than 4. When bigger values are used, however, the output gain is found to deviate much from the expected relation, being significantly smaller than the inverse proportional case. We can not explain this discrepancy since we do not understand how the gain adjusting is realized elec-

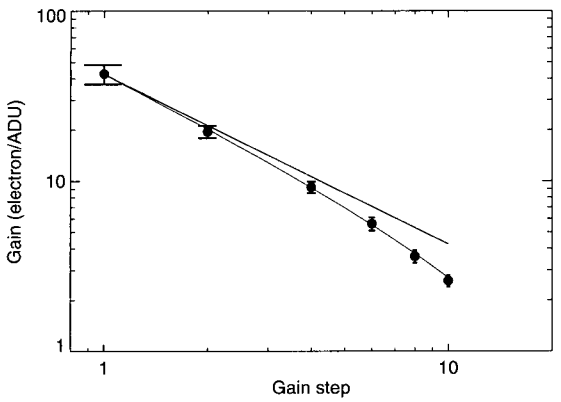

Fig. 7.— The input gain step versus the output gain. The line has been drawn to show the inverse proportional relationship.

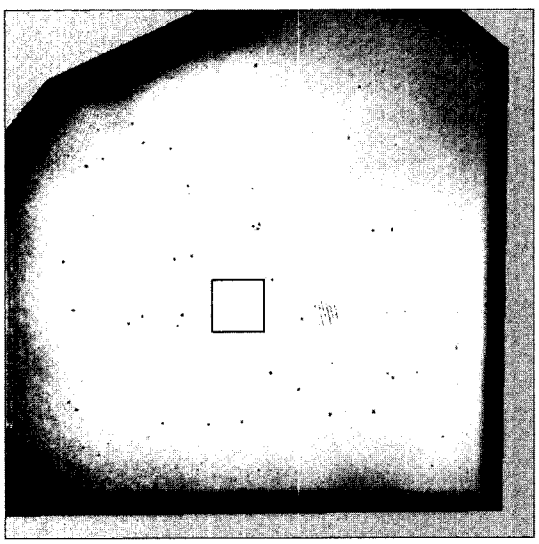

Fig. 8.— An example of the flat pattern of an observing system using the camera.

tronically.

The empirical relationship between the input gain step X and the gain g (in unit of electrons/ADU) is approximately described by the analytic expression

$$g = \frac{42.5}{X} \exp\left(-\frac{X-1}{20}\right). \quad (12)$$

(g) Flat Pattern

Figure 8 is an example of the flat pattern f_i of the observing system using the camera. The observing system consists of the 10 inch refractor in Big Bear Solar Observatory and the 1/4Å bandwidth H-alpha birefringent filter, and the DALSA 1M30P camera. To determine the flat pattern, we have applied a special technique developed by Chae (2004), which uses a number of relatively shifted images. The data were taken on 2004 August 3.

Note that the flat pattern depends not only on the characteristics of the CCD (such as quantum efficiency and charge transfer efficiency), but also on the characteristics of other parts comprising the observing system. For example, the darkening seen near the edges is the vignetting effect due to the limited field of view blocked by the internal field stop. Weak fringes are due to the interference between the light entering into the CCD window and that reflecting out of it. Dots and dirts are mostly due to the dust particles on the CCD window. Thus most conspicuous features seen in the flat image are not due to the relative gain of the camera.

To determine a measure of the pixel-to-pixel variation due to the non-uniformity of the CCD pixel only, we have chosen a small area as indicated by the box in the figure, in which other factors seem to contribute little to the variation. The standard deviation in this area is found to be about 1%.

V. SUMMARY

We have examined the performance and characteristics of the DALSTAR 1M 30P camera. The main results are summarized as follows.

1. The practically effective integration time is from 5 to 210 miliseconds.
2. The bias level is found to be 48.5±0.3 ADU except the region about 30 columns near the left edge.
3. The readout noise is about 1.3 ADU.
4. The dark current is about 8 ADU/s/pix.
5. The detector is linear with an accuracy better than 6 %.
6. The gain in the default mode is about 42 electrons/ADU.
7. The uniformity of the detector response appears to be better than 1%.
8. Applying binning appears to introduce additional electronic noise.
9. We found that there is a systematic discrepancy between the theoretical gain expected from the electronic adjusting and the empirically determined value from the noise characteristics.

The last two results suggest that operating the camera in the default mode may be the best since applying binning or increasing gain seems to be introducing additional electronic noise which we do not understand.

Summing up some characteristics of the DALSTAR 1M 30P camera such as dark current, dynamic range, linearity and gain appear to be inferior to the nighttime-purpose astronomical CCD cameras as studied, for example, by Park (1995) and Sung (1995). Nevertheless the camera is superior in its fast transfer speed of at

least 30 frame per second. This characteristic is very suited for solar observations. Previously video cameras were used for fast solar observations. But they have to be digitized for analysis, usually with a poor digital accuracy and big readout noises. Fast digital CCD cameras such as used in the present study are far better than video cameras when accurate measurements are required. The parameters we obtained for the 1M30P camera will be used as the basic inputs for the analysis of scientific data of the Sun in the forthcoming researches.

ACKNOWLEDGEMENTS

We appreciate the referee's constructive comments, which helped in clarifying the definition of gain. This work was supported by the Korea Research Foundation Grant (KRF-2002-015-CS0020).

REFERENCES

Chae, J. 2004, Flat-fielidng of Solar Hα Observations Using Relatively Shifted Images, Sol. Phys., 221, 1

Hanaoka, Y., Sakurai, T., Noguchi, M., & Ichimoto, K. 2004, High-cadence Hα imaging of solar flares, Advances in Space Research, 34, 2753

Howell, S. B. 2000, Handbook of CCD Astronomy, Cambridge University Press

Park, B.-G., Chun, M. Y., & Kim, S.-L. 1995, Laboratory Test of CCD #1 in BOAO, PKAS, 10, 67

Sung, H. 1995, The UBV CCD Photometry of Eight Young Open Clusters, PhD Thesis, Seoul National University

Wang, H., Qiu, J., Denker, C., Spirock, T., Chen, H., & Goode, P. R. 2000, High-Cadence Observations of an Impulsive Flare, ApJ, 542, 1080